Formation and Decomposition of Uranium–Oxygen Clusters in Fast Atom Bombardment of Dioxouranium(VI) Salts

Terence J. Kemp,* Keith R. Jennings and Paul A. Read
Department of Chemistry, University of Warwick, Coventry CV4 7AL, UK

Fast atom bombardment (FAB) of uranyl salts in involatile organic matrices produced a long series of clusters of general formula $[(UO_2)_xO_y]^+$ with x reaching nearly 40. For each value of x there is a series of values of y, with some value of y exhibiting the greatest abundance for each x value. Smaller clusters ($x \leqslant 22$) with even values of x show a stoichiometry of O:U of 2.5:1, while larger clusters ($x \geqslant 24$) show a reduced O:U ratio. All clusters with odd values of x adopt a O:U ratio of less than 2.5:1. Near $x = 24$, odd–even effects appeared in the relative intensities of the clusters. As $x \longrightarrow 40$ all cluster series tend to a final stoichiometry of O:U = 2.5:1. The collision-induced decomposition (CID) of $[(UO_2)_xO_y]^+$ produced long sequences of progressively smaller clusters *via* the loss of UO_2, UO_3 and UO_4 moieties; the detection of particular clusters depends on the collision-gas (argon) pressure. Odd–even alternation effects are apparent in the CID spectra. Clusters of general formula $[(ThO_2)_x]^+$ were produced by FAB of thorium(IV) nitrate, with x reaching 20; odd–even alternation effects are prominent when $x \geqslant 14$. The relatively complex behaviour exhibited by U–O clusters is associated with electronic effects, particularly the existence and relative stabilities of the +6, +5 and +4 oxidation states of uranium, as also manifested in U–O systems in the solid state, with which comparison can be made.

Aggregation processes leading to the formation of small clusters of metal atoms and of metal–oxygen and –ligand species detected mass spectrometrically are characteristic of the fast atom bombardment (FAB) of a number of simple salts and complexes of metals. Monomeric chelate complexes of Mg^{2+} were found to produce di- and tri-magnesium species featuring scrambling of the ligands when mixtures of magnesium chelates were used.[1] The ions Pb_2^+, Cu_2^+, $[Cu_2(OH)]^+$, $[Cu_2(OH)_2]^+$ and Cu_3^+ were detected on FAB of lead-based ceramic glasses.[2] The complex $[Pt(PPh_3)_4]$ gives small amounts of $[Pt_2(PPh_3)_n]^+$ ($n = 2$–4).[3] The FAB of simple ionic salts MX gives rise to a variety of $[(MX)_nM]^+$ and $[(MX)_nX]^-$ species of purely ionic nature.[4]

Many positive cluster ions of lanthanides (Ln) ranging from $[Ln_2O]^+$ to $[Ln_9O_{13}]^+$ have been reported by Selbin and co-workers[5] on FAB of a Schiff-base complex, as well as from simple salts. Later studies by the same group[6] focused on the collisionally induced decomposition (CID) of various yttrium oxide clusters. Small lanthanide–oxygen clusters have also been found in secondary ion mass spectrometric studies of macrocyclic complexes of lanthanide ions.[7] Bombardment of metals and metal oxides gives rise to series such as $[TiO(TiO_2)_n]^+$,[8] $[Ta_xO_y]^+$ ($x = 1$–6)[9] and $[U_xN_y]^+$ ($x = 1$–6).[9]

We have shown, in a preliminary note,[10] the ready formation of di-, tri-, tetra- and penta-uranium–oxygen cluster ions on FAB of uranyl salts, while Brown and Ismail[11] found clusters $[U_xO_y]^+$ with x up to 6 on FAB of uranyl dihydroxamates. In the present paper we describe the formation of a much larger family of $[U_xO_y]^+$ uranium–oxygen cluster ions produced by FAB or uranyl compounds with x up to 30, together with their collisionally induced decomposition.

The chemical aspects of FAB have been reviewed by Fenselau and Cotter[12] and the FAB of inorganic and organometallic compounds has been surveyed by Bruce and Liddell.[13] The occurrence of cluster species in mass spectrometry in general has been reviewed by Derrick[14] and by Kappes.[15]

Experimental

The mass spectra were obtained using two instruments, namely a modified MS-50 double-focusing instrument and a 'Concept' four-sector spectrometer supplied by Kratos Analytical Instruments.[16,17] Both of these utilise forward-geometry instrumentation and are fitted with a DS-90 data system. The bombarding atom beams were produced using a radially mounted Ion-Tech Ltd. saddle-field FAB gas gun. The Concept instrument consists of two horizontal forward-geometry mass spectrometers connected *via* a collision cell,[18] termed a 'flexicell', in which ion–molecule collisions can be effected.

The ions produced at the FAB probe tip were accelerated to 8 keV (*ca.* 1.28×10^{-15} J) and focused into a narrow beam before entering the mass spectrometer. Ion currents were optimised by using a cooled probe tip of 5 mm diameter and by adjusting both the source pressure and the quantity of matrix used. In general, high source pressures gave superior signal-to-noise ratios for lower clusters but tended to supresss higher clusters, possibly as a result of collision-induced decomposition. For the mass ranges studied, calibration errors of up to 2 mass units in 2000 (see schemes of fragmentation below) were regarded as acceptable.

Results

General Features.—The positive-ion FAB mass spectrum of uranyl nitrate dissolved in the minimum of water and then made up in a sulfolane (tetrahydrothiophene 1,1-dioxide) matrix is shown in Fig. 1. This shows: (*i*) the appearance of U–O species at relative molar mass values of up to 7000 implying up to at least 26 U atoms in the cluster; (*ii*) the existence of a long series of pronounced maxima at regular mass intervals corresponding to the addition of UO_2 and UO_3 moieties; (*iii*) a well developed substructure associated with each of these maxima, which is associated with a range of U–O stoichiometries about the principal value within each group; (*iv*) a smooth decline in the intensity of each maximum on going from low to high mass.

All the many species present in Fig. 1 are attributable to clusters of formula $[(UO_2)_xO_y]^+$ and closer examination of these revealed the following: (*a*) the amount of 'excess' oxygen, measured by y, increases with increasing cluster size x; (*b*) careful measurements at high mass using the first two sectors of

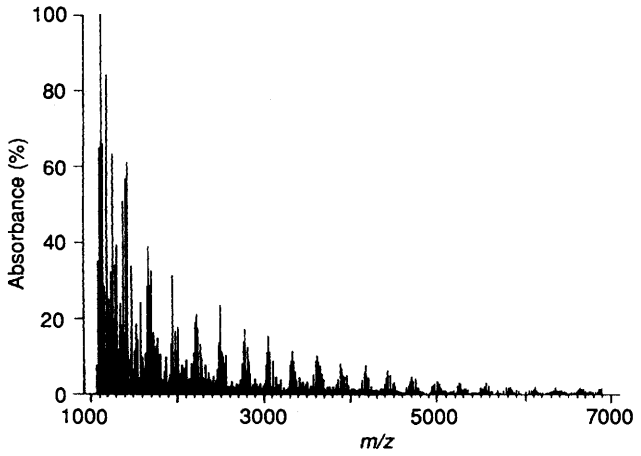

Fig. 1 The FAB mass spectrum of uranyl nitrate (sulfolane matrix)

the Kratos Concept instrument revealed that the series extends continuously until x reaches 37, although there was evidence for a few isolated even higher values of x; (*c*) while there is a general trend for successive members of the series $[(UO_2)_xO_y]^+$ to decrease exponentially in intensity as x increases, there are 'abnormalities', either positive or negative, in the region of x = 9, 14–16, 19–22, 25, 27 and 32; (*d*) there is some evidence for odd/even alternation at higher values of x; (*e*) matrix adducts were observed when certain matrices (dimethyl sulfoxide, glycerol, 3-nitrobenzyl alcohol) were employed, being particularly marked at low values of x (indeed the matrix appeared to promote the formation of low-mass species); adducts were also detected, albeit with lower abundances, at high values of x, *e.g.* at 23–30 for $[(UO_2)_xO_{11}$·matrix$]^+$.

Stoichiometry of Clusters.—Further to the general observations made above, a quantitative examination of the cluster stoichiometry revealed the following. A plot y *versus* x for the most intense member of each family of clusters $[(UO_2)_xO_y]^+$ shows the clusters to fall into three groups, represented in Fig. 2 by three parallel lines. These groups can be represented by equations (1) [odd values of x (except 27)], (2) [even values of x (2–16, 20, 22 and 28)] and (3) [even values of x (18, 24, 26 and 30–36)]. Thus smaller clusters with even values of x prefer a stoichiometry of $UO_{2.5}$ while large clusters display a reduced O:U ratio. All clusters with odd values of x adopt a O:U ratio less than 2.5:1 irrespective of cluster size, which is intermediate between the two values found with even-x clusters.

$$y = 0.5x - 0.5 \quad (1)$$

$$y = 0.5x \quad (2)$$

$$y = 0.5x - 1.0 \quad (3)$$

Two further graphical treatments of the cluster intensity data are revealing. In Fig. 3 is plotted the variation of the O:U ratio (denoted by z) *versus* cluster size, measured by x. All the odd-x clusters fall on a single curve which tends asymptotically to z = 2.5 as x tends to infinity, in accordance with equation (1). The even-x clusters fall into two groups, in line with equations (2) and (3), with the smaller clusters showing z = 2.5 and the larger clusters deviating initially more strongly from z = 2.5, but nonetheless approaching z = 2.5 as x becomes very large. These curves can be linearised, and in Fig. 4 the plot of z *versus* $1/x$ shows three linear dependences, for odd values of x [equation (4)], small, even values of x [(5)] and larger, even values of x [(6)]. Thus small ($x \leqslant 12$) even-x clusters and very large ($x > 50$) even-x clusters exhibit a O:U ratio (z value) of 2.5:1, while those of intermediate size show $z < 2.5$.

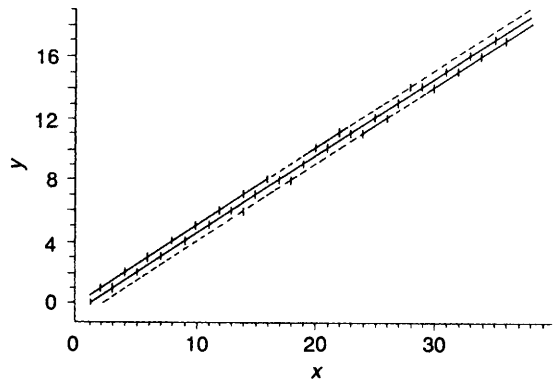

Fig. 2 Variation of y in $(UO_2)_xO_y$ with cluster size as measured by x

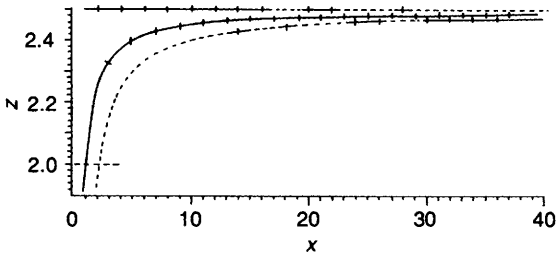

Fig. 3 Variation of O:U ratio (denoted by z) with cluster size as measured by x

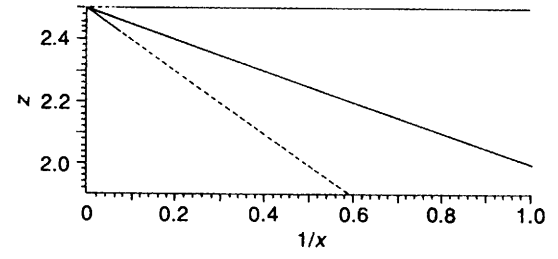

Fig. 4 Graphical representation of the variation in O:U ratio (z) with reciprocal cluster size ($1/x$)

$$z = -(0.5/x) + 2.5 \quad (4)$$

$$z = 2.5 \quad (5)$$

$$z = -(1/x) + 2.5 \quad (6)$$

The dependence of cluster stoichiometry on cluster size, especially for even-x clusters, suggests that the clusters adopt different structural arrangement over different ranges of size. Small even-x clusters adopt a stoichiometry $UO_{2.5}$, with their neighbouring odd-x clusters exhibiting stoichiometries between UO_2 and $UO_{2.5}$. However, at intermediate sizes, the even-x clusters feature lower O:U ratios. Near x = 24 the even-x clusters show slightly lower relative intensities than do their odd-x neighbours.

The tendency of both odd- and even-x clusters to approach a common stoichiometry of O:U = 2.5:1 at high values of x suggests that the structure of these large clusters may be related to those of the U_2O_5 phases,[19] of which three are known, α (unknown crystal symmetry), β (hexagonal fluorite) and γ (monoclinic). These phases mark the changeover between fluorite-type structures to those containing predominantly uranyl-type bonding.[19] The UO_2–UO_3 phase diagram is characterised by a range of well defined U:O compounds between O:U stoichiometries of 2.0 and 2.5:1 including U_8O_{19} (z = 2.375), $U_{16}O_{37}$ (2.312) and U_4O_9 (2.25). The contrasting simplicity of the FAB mass spectra of thorium salts (see below)

is related to the simplicity of the Th–O system for which ThO_2 is the only stable oxide species.

Collision-induced Decomposition of Uranyl Clusters.—(*i*) *Octauranyl clusters.* The CID spectra for members of the octauranyl species $[(UO_2)_8O_y]^+$ were determined at various argon pressures. Under single-collision conditions (beam transmission 70%) the spectrum for $[(UO_2)_8O_6]^+$ is characterised by the appearance of daughter clusters consistent with the loss of UO_3 units. At higher argon pressures (beam transmission 50%), a long sequence of daughter clusters is found with x from 8 down to 1. The heavier members lose UO_3 units but once the O:U ratio reaches 2:1 then UO_2 units are lost. At still higher argon pressures the lighter clusters lost various combinations of UO_2 and UO_3 units, the daughter clusters showing O:U > 2.0:1. At 30% beam transmission the loss of UO_4 was observed as an additional pathway; Fig. 5 illustrates the sequence in Scheme 1.

The most abundant ions were found at low collision-gas pressures, when UO_3 loss was the dominant pathway, which indicates this to be the lowest-energy route. A CID spectrum of $[(UO_2)_8O_4]^+$ gave generally similar behaviour. A prominent feature of Fig. 5 is the even–odd alternation, *i.e.* the U_7, U_5, U_3 and U species are more abundant that their neighbouring U_8, U_6, U_4 and U_2 analogues, and this pattern was repeated for all octauranyl clusters studied.

(*ii*) *Heptauranyl clusters.* As with the octauranyl clusters, the general behaviour was for increased collision-gas pressures to promote more extensive fragmentation and additional pathways. The dominant pathway for the six series of clusters examined (x = 7, y = 0–6) involved the initial loss of UO_3 units followed, when O:U = 2.0:1, by the loss of UO_2 units. Some exceptions to this general pattern were found as follows.

For $[(UO_2)_7O_5]^+$ the daughter fragments with x = 5 were found to dissociate by loss of UO_4 units to form $[(UO_2)_4O_2]^+$ over a range of collision-gas pressures. The relative abundances of the x = 1, 3 and 5 clusters were found to be enhanced over a range of collision-gas pressures. The ion $[(UO_2)_7O_5]^+$ itself displayed rather low abundances of fragment ions at low collision-gas pressures (70% transmittance), with an exponential decrease in abundance with decreasing cluster size, and with clusters x = 1–3 being absent. At 50% beam transmittance all clusters x = 1–6 were apparent, but with particularly low abundances for 1, 2 and 4 (*i.e.* the x = 3 and 5 clusters are especially stable towards fragmention). Fig. 6 shows that at 30% transmittance this odd–even alternation is well developed, and at 10% the effect was further enhanced. The fragmention sequence in Fig. 6 is shown in Scheme 2.

For $[(UO_2)_7O_4]^+$ the x = 3 and 5 daughter clusters had greater relative intensities, and the x = 1 and 2 daughters became significant only at high gas pressures; $[(UO_2)_7O_y]^+$ (y = 1–3) also featured stepwise loss of UO_3 and UO_2 units and a pronounced odd–even alternation in abundance at high pressures. At high collision-gas pressures (parent beam transmittance 10%) the x = 6 daughter ion became significantly weaker in abundance, while the intensities of the daughters $[(UO_2)_xO_2]^+$ became more significant for x = 3–5. This loss of U atoms or UO species becomes the preferred route in this series.

The general trend in the heptauranyl clusters is for loss of UO_3 to occur from larger species, while once a daughter achieves a stoichiometry $[(UO_2)_7]^+$ then UO_2 units are eliminated.

(*ii*) *Hexauranyl clusters.* These show the same general behaviour as that of heptauranyl clusters as shown in Fig. 7, from which the even–odd alternating intensity effect is clearly

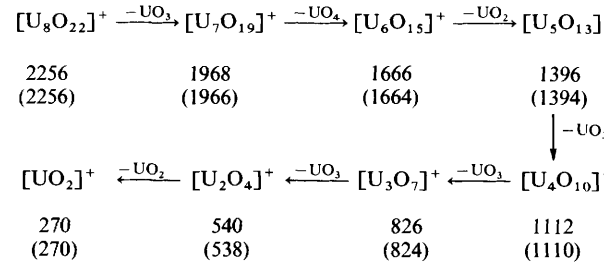

Scheme 1 Numbers in parentheses are theoretical m/z values

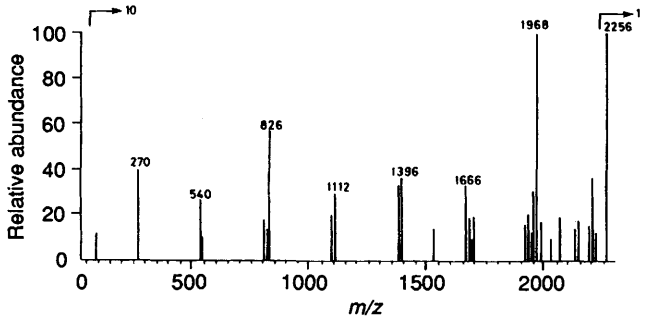

Fig. 5 The CID spectrum for $[(UO_2)_8O_6]^+$ (m/z = 2256); collision gas argon (30% beam transmittance), Flexicell at 2 kV

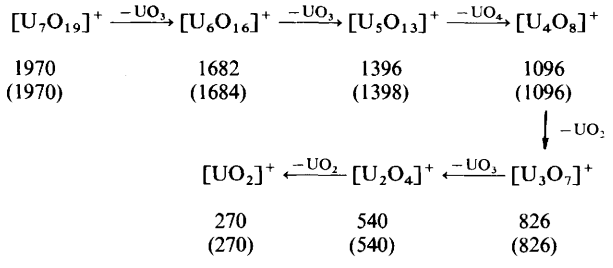

Scheme 2

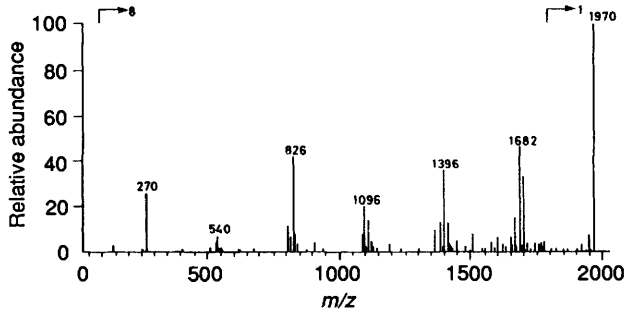

Fig. 6 The CID spectrum for $[(UO_2)_7O_5]^+$ (m/z = 1970); conditions as in Fig. 5

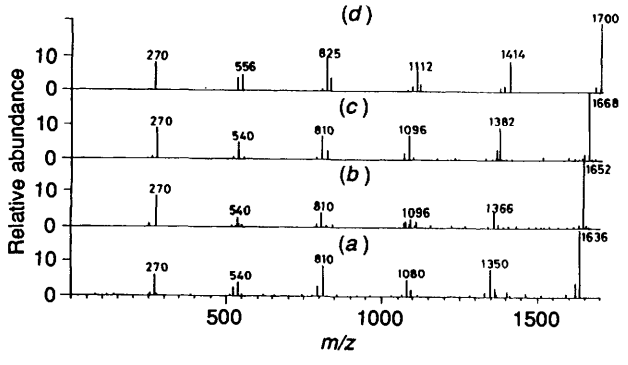

Fig. 7 The CID spectra for $[(UO_2)_6O_y]^+$ [y = 1 (*a*), 2 (*b*), 3 (*c*) or 5 (*d*)] conditions as in Fig. 5

visible. The pattern of daughter clusters originating from $[(UO_2)O_6]^+$ summarised in Table 1 reveals that increase in the collision-gas pressure results in a systematic relative increase in the abundances of more extensively fragmented species. The odd–even alternation effect is found at all collision-gas pressures but with minor modification (Fig. 8).

The ion $[(UO_2)_6]^+$, like $[(UO_2)_7]^+$, displays some tendency to eliminate UO units, thus it eliminates either UO_2 or UO to form $[(UO_2)_5]^+$ and $[(UO_2)_5O]^+$ respectively. At higher collision-gas pressures no $x = 5$ species were detectable and the spectrum became dominated by tetrauranium daughter ions.

Penta- and tetra-uranyl clusters. These followed a generally similar fragmentation pattern. The triuranyl daughter clusters were relatively enhanced, and the diuranyl clusters diminished, at higher collision-gas pressures. Each tetrauranyl cluster decomposed to a variety of $[(UO_2)_3O_y]^+$ species.

Discussion

The initial mode of decomposition of the parent clusters $[(UO_2)_xO_y]^+$ is elimination of a neutral UO_3 unit: $[(UO_2)_xO_y]^+ \longrightarrow [(UO_2)_{x-1}O_{y-1}]^+ + UO_3$. This single process is dominant at low collision-gas pressures, but as the pressure is increased further fragmentations are undergone by the parent and daughter clusters until the O:U stoichiometry nears 2.0:1, and thereafter the main pathways becomes elimination of UO_2 units. At very high collision-gas pressures the elimination of UO_2 begins at increasingly large daughter cluster sizes, and loss of UO_4 is sometimes found. For a fixed argon pressure the larger clusters fragment more readily.

Increase of the collision-gas pressure also enhances the odd–even alternation effect in the ion abundances, with $x = 3$ clusters being conspicuously stable. The extent and ease of fragmentation is also related to the y value, thus with $[(UO_2)_6O_y]^+$ a high value of y (higher O:U ratio) is associated with more extensive fragmentation compared with clusters with a low y value.

The sequence of dominant clusters species detected during CID experiments for the different values of x can be represented graphically: Fig. 9 shows those observed values of y for a given value of x. Fig. 10 shows how the O:U ratio (denoted by z) varies with $1/x$ for the various fragmentation pathways, indicating that all the cluster sequences originate from an imaginary infinitely large cluster with $z = 3.0$, *i.e.* a UO_3 phase.

The complexity of the FAB and CID mass spectra of U–O clusters is associated with electronic effects, particularly the

Table 1 The variation in % internal reference for the daughter clusters of $[(UO_2)_6O_5]^+$ at 30, 20 and 10% transmittance

		% Internal reference		
Species	*m/z*	30	20	10%
$[(UO_2)_5O_5]^+$	1700	100.0	100.0	70.2
$[(UO_2)_5O_4]^+$	1414	7.4	15.2	19.6
$[(UO_2)_5O_3]^+$	1398	1.5	8.5	8.2
$[(UO_2)_4O_3]^+$	1128	2.5	10.7	21.8
$[(UO_2)_4O_2]^+$	1112	4.3	6.3	11.9
$[(UO_2)_3O_2]^+$	842	3.7	13.8	20.9
$[(UO_2)_3O]^+$	826	7.6	21.3	33.3
$[(UO_2)_2O]^+$	556	3.8	13.0	25.1
$[(UO_2)_2]^+$	540	3.2	19.5	14.0
$[(UO_2)]^+$	270	7.0	55.6	100

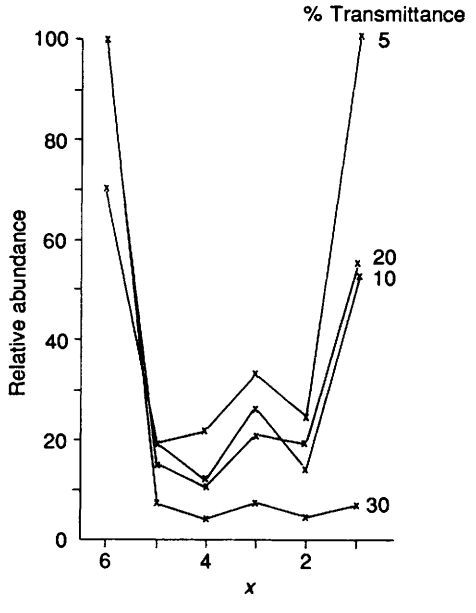

Fig. 8 Variation in relative intensity of the daughter-ion cluster from CID with decreasing cluster size x for a range of collision-gas pressures (measured by percentages of beam transmittance)

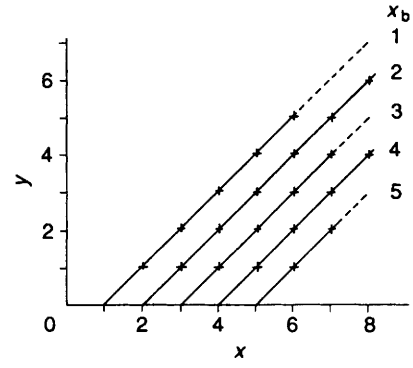

Fig. 9 Graphical representation of the dominant CID fragmentation pathways: each sloping line represents a sequence of species of stoichiometry $[(UO_2)_xO_y]^+$ where x decreases to an ultimate value x_b

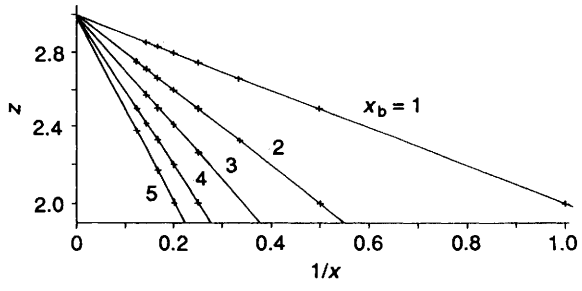

Fig. 10 Graphical representation of the dominant CID fragmentation pathways: dependence of O:U ratio (z) on reciprocal cluster size ($1/x$)

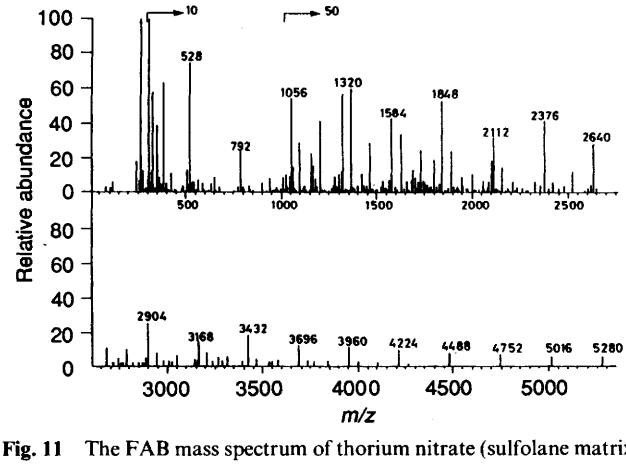

Fig. 11 The FAB mass spectrum of thorium nitrate (sulfolane matrix)

existence of established oxidation states of U of +3, +4, +5 and +6.[20]

Thorium–Oxygen Clusters.—The FAB of a variety of thorium(IV) salts (see Fig. 11) led to production of a long series of cluster ions $[(ThO_2)_x]^+$ with $x \leqslant 14$. The lower-mass clusters show the presence of peaks due to oxygen-deficient species $[(ThO_2)_x(ThO)_y]^+$ and also matrix adducts. An alternation effect was apparent for clusters with relative molar mass < 3700, but above this figure abundances of $(ThO_2)_x$ clusters decreased exponentially. The relative simplicity of the FAB picture with Th–O clusters is associated with the lack of stable oxidation states other than +4.[20]

Acknowledgements

P. A. R. thanks the SERC for the award of a studentship.

References

1 P. R. Ashton, D. E. Fenton, R. N. Prasad, M. Jindal and M. Jain, *Inorg. Chim. Acta*, 1988, **146**, 99.
2 G. G. Dolnikowski, J. T. Watson and J. Allison, *Anal. Chem.*, 1984, **56**, 197.
3 R. Davis, I. F. Groves, J. L. A. Durrant, P. Brooks and I. Lewis, *J. Organomet. Chem.*, 1983, **241**, C27.
4 C. Javanaud and C. Eagles, *Org. Mass. Spectrom.*, 1983, **18**, 93.
5 I. A. Kahwa, J. Selbin, T. C.-Y. Hsieh and R. G. Laine, *Inorg. Chim. Acta*, 1988, **141**, 131.
6 I. A. Kahwa, J. Selbin, T. C.-Y. Hsieh, D. W. Evans, K. M. Pamidimukkala and R. G. Laine, *Inorg. Chim. Acta*, 1988, **144**, 275.
7 S. Daolio, B. Facchin, C. Pagura, P. Guerriero, S. Sitran and P. A. Vigato, *Inorg. Chim. Acta*, 1990, **178**, 131.
8 W. Yu and R. B. Freas, 36th American Society for Mass Spectrometry Conference, San Francisco, 1988.
9 F. M. Devienne, R. Combarieu and M. Teisseire, *Surf. Sci.*, 1981, **106**, 204.
10 K. R. Jennings, T. J. Kemp and P. A. Read, *Inorg. Chim. Acta*, 1989, **157**, 157.
11 D. A. Brown and S. Ismail, *Inorg. Chim. Acta*, 1990, **171**, 41.
12 C. Fenselau and R. J. Cotter, *Chem. Rev.*, 1987, **87**, 501.
13 M. I. Bruce and M. J. Liddell, *Appl. Organomet. Chem.*, 1987, **1**, 191.
14 P. J. Derrick, in *Advances in Mass Spectrometry*, 1985, ed. J. F. J. Todd, Wiley, Chichester, 1986, p. 85.
15 M. M. Kappes, *Chem. Rev.*, 1988, **88**, 369.
16 K. R. Jennings and G. Dolnikowski, in *Mass Spectrometry, Methods in Enzymology*, ed. J. J. McCloskey, Academic Press, 1990, vol. 193, p. 37.
17 M. L. Gross, in *Mass Spectrometry, Methods in Enzymology*, ed. J. J. McCloskey, Academic Press, 1990, vol. 193, p. 131.
18 R. K. Boyd, *Int. J. Mass Spectrom. Ion Process.*, 1987, **75**, 243.
19 H. R. Hoekstra, S. Siegal and F. X. Gallagher, *J. Inorg. Nucl. Chem.*, 1970, **32**, 3237.
20 F. A. Cotton and G. Wilkinson, *Advanced Inorganic Chemistry*, 4th edn., Wiley, New York, 1980, pp. 1204–1026; Gmelin, *Thorium und Isotope*, Verlag Chemie, Weinheim, 1955, pp. 77–81.

Received 11*th November* 1994; *Paper* 4/06876I